# High photocatalytic performance of coated TiO$_2$ layers assisted by H$_2$O$_2$ oxidizing agent to remove an azo dye from water via the synergistic effect of optimum conditions

Azeddine Bouarioua

*Faculty of Engineering, Department of Process Engineering, Laboratory of Environmental Engineering, University of Badji Mokhtar, P.O. Box: 12, 23000 Annaba, Algeria, Tel./Fax: +213 38 87 65 60; email: azeddine.bouarioua@gmail.com*

## ABSTRACT

UV/H$_2$O$_2$, UV/TiO$_2$, and TiO$_2$/UV/H$_2$O$_2$ processes with three immobilized catalyst layers were applied in a batch photocatalytic reactor to eliminate methyl orange (MO) azo dye as a model organic pollutant. The aim of this article is to improve the performance of oxidation systems in terms of efficiency and rapidity for the organic pollutant removal and to optimize the oxidant to contaminant molar ratios. In all applied processes, the dye oxidation kinetic has well followed the first-order model. In the UV/TiO$_2$ process, the elimination of MO was found 5 times more rapid under optimum conditions than that under initial conditions. The experiments revealed two optimum values of $[H_2O_2]_0/[MO]_0$ molar ratios. These were 587 and 352 for UV/H$_2$O$_2$ and TiO$_2$/UV/H$_2$O$_2$ systems, respectively. Under optimum conditions, TiO$_2$/UV/H$_2$O$_2$ produced total dye color removal and 88.9% total organic carbon reduction in 10 min of reaction. The synergistic effect of immobilized layers of TiO$_2$ catalyst and optimum H$_2$O$_2$ oxidizing agent intensively enhanced the generation of OH$^•$ powerful oxidant and the separation of photoexcited electron-hole pairs. The optimum TiO$_2$/UV/H$_2$O$_2$ as a high-performance photocatalytic system can be helpful in the removal of organic contaminants from water.

*Keywords:* Water treatment; Organic pollutant; Azo dye removal; Photocatalytic performance; Coated TiO$_2$ layers; Synergistic effect; Optimum conditions; Oxidant to contaminant molar ratio

## 1. Introduction

The worldwide concern for the development of alternative water reuse technologies, mainly focused on agriculture and industry is continually increasing [1]. Over the years, it has been observed that certain pollutants cannot be treated by biological and conventional treatment methods because of their high chemical stability or strong resistance to mineralization [2]. In such cases, it has been necessary to adopt more reactive and efficient chemical treatment processes. A group of oxidation technologies defined as advanced oxidation processes (AOPs) which operate at ambient temperature and pressure has gained prominence as alternative treatment methods [2]. These processes have the potential ability to mineralize most of the organic contaminants into carbon dioxide and water [3]. The basic principle of AOPs involves the production of hydroxyl radicals (OH$^•$), which can be generated from hydrogen peroxide (H$_2$O$_2$), ozone, photocatalysis, or oxidants in combination with using ultraviolet (UV) radiation. In some cases, two or more radical generators are used in combination. However, it is the OH$^•$ that is mainly responsible for the degradation of organic compounds [4]. Specifically, the UV/H$_2$O$_2$ method uses UV–C photons to photolyze H$_2$O$_2$ and produce OH$^•$ [4]. The photolysis of H$_2$O$_2$ at 254 nm yields the formation of two OH$^•$ per photon absorbed [5] whereas the absorption of photon energy (hν) equals or exceeds the band gap of the TiO$_2$ semiconductor photocatalyst generating electron-hole pairs [6]. The excited electron and hole move to the surface of the TiO$_2$ and react with adsorbed substances; the holes can oxidize OH$^-$ ions

and $H_2O$ molecules into reactive radicals or react directly with pollutants in the water [7]. In the $UV/H_2O_2$ process, $OH^\bullet$ is formed in the liquid phase and can directly react in solution. $TiO_2$ is a solid catalyst where $OH^\bullet$ radicals are formed on its surface. Therefore, the adsorption of organics on the surface of $TiO_2$ particles is critical and is the determining step of UV photocalysis [7].

A practical problem in the use of $TiO_2$ as photocatalyst is the undesired electron–hole recombination, which in the absence of the proper electron acceptor or donor, it is extremely efficient and thus represents the major energy-wasting step, thereby limiting the achievable quantum yield [8]. They have opined that the strategy to inhibit electron–hole recombination is to add irreversible electron acceptors to the reaction system [8].

Hydrogen peroxide is considered to be environmentally friendly as it is composed only of oxygen and hydrogen atoms and it could promote photocatalysis in two ways [9,10]. Firstly, the reduction of $H_2O_2$ at the conduction band would produce hydroxyl radicals. Secondly, the direct self-photocleavage by UV irradiation would also produce hydroxyl radicals [9,10]. Thus, hydrogen peroxide can be used as an efficient electron acceptor and may efficiently improve the photocatalytic process. Aiming at further enhancement of the photocatalytic reactions to eliminate the highly colored wastewater by ensuring the inhibition of the electron–hole recombination effect, the attention should be focused on the benefits of the presence of $H_2O_2$ in the $TiO_2$ photocatalysis system.

A big effort has been made to study the effect of hydrogen peroxide and various factors on the photocatalytic process of removing organic pollutants from water. The majority of studies have attempted to improve the photocatalytic performance of titanium dioxide by the use of suspended catalysts, novel composites or doping $TiO_2$ photocatalyst with metal oxides. However, they merely have focused on the color removal of dyes and no information about the degradation and mineralization of organic compounds was left at the end of photocatalytic processes. Kang et al. [11] concluded nearly 60% of decolorization of Rhodamine B dye solution (10 mg/L) was obtained after 210 min of visible-light irradiation by ($H_2O_2$ + 50 mg suspended $TiO_2$ P25) system. Zhiyong et al. [12] studied the effect of adding $H_2O_2$ to a suspension of $TiO_2$ Degussa P25 (0.5 g/L) on the decolorization of methyl orange (MO) under sunlight irradiation. The experiments revealed an optimum addition of 1 mM $H_2O_2$ for color removal of dye solution in 1 h. Egerton et al. [13] concluded that the decolorization of anionic azo-dye reactive orange 16 by UV-C irradiation of $H_2O_2/TiO_2$ (2 g dm$^{-3}$, 20 mM $H_2O_2$) was about 5 times faster than that by the $TiO_2$ photocatalyzed reaction. Huayue et al. [14] indicated that 99.5% of MO aqueous solution (15 mg/L, pH 6.0) was successfully decolorized after 130 min of simulated solar light irradiation in the presence of 1.0 g/L hexagonal CdS nanocrystals/anatase $TiO_2$/polymer nanocomposite thin films and 3.9 mmol/L $H_2O_2$. Niu and Hao [15] also prepared nanocomposite films of titanium dioxide ($TiO_2$)/polyoxometalate, decatungstate ($Na_4W_{10}O_{32}$, abb. $W_{10}O_{32}$) by electrostatic layer-by-layer self-assembly method. They indicated that the addition of hydrogen peroxide with concentration over the range 2.5–20 mM to the nanocomposite films evidently improves the decolorization rate of MO (10 mg/L)

by inhibiting the electron–hole recombination and producing an abundance of $OH^\bullet$ radicals. The addition of both the efficient electron acceptors of polyoxometalates (POMs) and the irreversible electron acceptor $H_2O_2$ (20 mM) to the $TiO_2$ system produced more than 96.00% of MO color removal within 30 min. Huang et al. [16] reported that the decolorization of MO solution under sunlight irradiation by Pt modified $TiO_2$ loaded on natural zeolite reached the maximum (about 92%) after 30 min by adding 1.5 mM/L of $H_2O_2$.

The oxidation of azo dyes can lead to the formation of harmful intermediates, which are more toxic than the initial compounds [17]. Complete decolorization of the dye solution does not mean that the dye is completely mineralized [18]. For this reason, it is imperative to evaluate the mineralization level induced by the UV photocatalysis processes.

In the literature, there are few reports focus on the mineralization of organic dyes. Nevertheless, they have not been achieving high performance of mineralization of organic molecules regarding the importance of rapid photocatalytic processes to deal with contaminated effluents. Kulkarni and Thakur [19] reported that when an optimum $H_2O_2$ (0.375g) was added to suspended $TiO_2$ (100 mg), a complete decolorization and 65% total organic carbon (TOC) reduction of Navy Blue HE2R diazo dye ($2.5 \times 10^{-5}$ mol/L) were achieved in 2 h of UV irradiation. Dharmarajan et al. [20] studied the photocatalytic degradation of reactive dyes over Cu-doped $TiO_2$ nanocrystals and direct sunlight. Total color removal of 50 mg/L solutions of dyes achieved after 2 h at pH 5 with a catalyst dosage of 1 g/L and $H_2O_2$ oxidant (1 mM). However, only 67.2% (Reactive blue 4), 64.1% (Reactive red 120), 70.5% (Reactive black 5) and 76.3% (Reactive orange 30) of chemical oxygen demand (COD) reduction were obtained. Thus, the mineralization of dyes takes place at a slower rate when compared to the decolorization of the dyes. Soutsas et al. [21] reported the decolorization and degradation of four commercial reactive azo dyes (Remazol Red RR, Remazol Yellow RR, Procion Crimson H-EXL and Procion Yellow H-EXL) via $TiO_2/UV/H_2O_2$ heterogeneous photocatalytic process. Under optimum parameters (suspended $TiO_2$ = 1 g/L, $[dye]_0$ = 75 mg/L, $[H_2O_2]_0$ = 0.1%w/w and pH 3), almost 100% of decolorization of all dyes reached in 25 min. However, degradation proceeds much slower than decolorization. COD removal achieved after 4 h of UV irradiation.

The previous paper [22] has evaluated the photocatalytic activities of three stable immobilized layers of $TiO_2$ powder under UV irradiation for the decolorization of MO aqueous solution MO as a model organic contaminant. The new work aims to enhance the photocatalytic performance of $UV/TiO_2$, $UV/H_2O_2$ and $TiO_2/UV/H_2O_2$ systems in terms of efficiency and rapidity for the mineralization and decolorization of MO azo dye pollutant. This work focuses on the synergistic effect of optimum conditions together, especially the presence of coated layers of $TiO_2$ photocatalyst with highly active sites and hydrogen peroxide as a powerful electron acceptor and hydroxyl radicals production. These favorable conditions may ensure the generation of hydroxyl radicals with highly photonic efficiency to oxidize and remove organic compounds. In addition, this study discusses the photocatalytic oxidation of organic compounds in the aqueous medium and finds out the optimum initial concentration of hydrogen peroxide in each of $UV/H_2O_2$ and $TiO_2/UV/H_2O_2$ processes.

To my knowledge, for the first time, the present paper investigates the relationship between the pollutant and oxidizing agent in the presence of immobilized catalyst layers and determines the optimum oxidant to contaminant molar ratio.

## 2. Experimental setup

### 2.1. Materials

MO powder ($C_{14}H_{14}N_3NaO_3S$, molecular weight 327.34 g/mol) was purchased from Fluka (Bucharest, Romania). Degussa P25 titanium dioxide powder (mainly anatase with a specific surface area of 50 $m^2$/g and a mean particle size of 30 nm) from Sigma-Aldrich (Allemagne). Ethanol ($C_2H_5OH$, 96Vol.%) and nitric acid ($HNO_3$), were supplied by Sigma-Aldrich. The nitric acid was used to adjust the pH of the deposition suspension. Acetone ($C_3H_6O$, 99.5%) was obtained from Cheminova Internacional (Spain). Hydrogen peroxide aqueous solution ($H_2O_2$, 30%) was purchased from Biocheme Chemopharma (France) and was used as received.

MO azo dye in the aqueous solution (Fig. 1) is used as a model organic pollutant.

### 2.2. Preparation and characterization of TiO₂ films

In this study, three stable, repeatable layers of $TiO_2$ powder immobilized on glass by the easy dip-coating technique are used as a catalyst. The glass slides made from Citogla, England with a surface of 7.5 $cm^2$ (25 mm × 30 mm) were sonicated for 15 min, with successively distilled water, acetone, and ethanol, to remove impurities from substrates. Then they were dried at 80°C and weighed before any coating by using digital balance to determine the initial weight of the substrate.

The film was prepared by suspending 3 g of $TiO_2$ powder in 60 mL of 30/70% (w/w) methanol/water mixture, which was sonicated for 15 min to obtain a better dispersion of $TiO_2$ particles in the suspension. This was followed by adding dilute nitric acid (0.1 N) to adjust the pH of the suspension at pH 3 (Hanna pH-meter, Germany) in order to obtain strong adhesion between $TiO_2$ and the support. Therefore, it is expected that there is an electrostatic attraction between the two surfaces that will enhance the adhesion. The whole suspension was vigorously stirred for 1 h to prevent the particles aggregate of $TiO_2$ and ensure its full dispersion. As a precaution, the vigorous stirring of the suspension was maintained

until the deposition step to avoid the reproduction of the sedimentation.

The nanocrystalline film was immobilized on glass substrates by easy dip-coating technique. The glass slide was dipped into the solution for 1 min and then withdrawn manually in order to form a stable deposition of $TiO_2$ film. The film was dried in ambient for 12 h and then heated in a furnace at 500°C for 2 h to secure adhesion between the $TiO_2$ film and the glass substrate, and also to remove all organic components from the film. Afterward, the coated film was washed in distilled water to remove unattached $TiO_2$ particles from the support surface and dried in ambient for 6 h and in a drying room for 15 min; after that, the samples were weighed to determine the amount of $TiO_2$ powder-coated on the glass substrate.

The dip-coating procedure was repeated more times to obtain a multilayer of $TiO_2$ powder with an increased amount of coated catalyst.

The X-ray diffraction (XRD) analysis was performed on a PANalytical (Netherlands) (X'Pert Pro MPD) powder diffractometer equipped with X'Celerator detector, using Cu K$\alpha$ X-rays ($\lambda$ = 0.154 nm, 40 kV, 30 mA, 20°–80° 2θ range; data recorded at 0.017° step size, 6.985 s/step). The observation of the morphology of the coated films was carried out using a scanning electron microscopy FEI QUANTA 200 FEG: FEI Co., Inc., Hillsboro, Oreg, USA.

### 2.3. Photocatalytic reactor

The photocatalytic tests were performed in a self-made reactor. As illustrated in Fig. 2, the photocatalytic reactor is an open cylindrical batch thermostatic reactor with a double envelope made of glass with an internal diameter of 7.5 cm. The photoreactor was housed by a closed self-designed box to concentrate the light photons toward the dye solution surface inside the double envelop reactor and also to avoid the radiation risks. The irradiation was performed using three artificial UV lamps with a double tube of 15 W (Vilber Lourmat, France). The UV lamps were separately fixed on the internal sides of the self-designed box around and parallel to the double envelope reactor with equal distances (*d*) of 2 cm. The intensity of the UV radiation (*I*) was measured by a UV radiometer (VLX-3W, from Vilbert Lourmat, France). For the UV/$TiO_2$ process only, three UV lamps of 365 nm were used [4,5,15,23]. However, for both UV/$H_2O_2$ and $TiO_2$/UV/$H_2O_2$ processes, three UV lamps of 254 nm were used [5,15,22]. It has been reported that although $TiO_2$ particles are activated
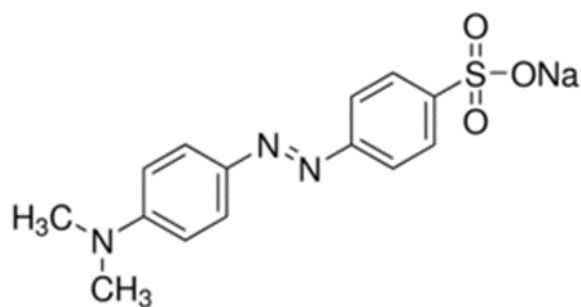


| Chemical formula | $C_{14}H_{14}N_3NaO_3S$ |
| Molecular weight | 327.33 g mol$^{-1}$ |
| C.I number | 13025 |
| CAS number | 547-58-0 |

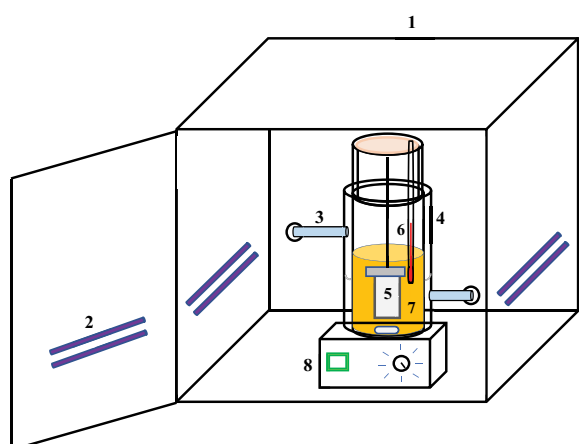Fig. 1. Molecular structure and characteristics of MO azo dye.

Fig. 2. Schematic of the photocatalytic reactor. (1) Irradiation box; (2) UV lamps with a double tube of 15 W; (3) cooling water; (4) glass double envelope reactor; (5) TiO$_2$ films-coated glass; (6) thermometer; (7) MO solution with a magnetic stirring bar; (8) magnetic stirrer.

at wavelengths < 380 nm [5] and H$_2$O$_2$ cannot be photolyzed at wavelengths higher than 280 nm [7,24] and still enables the activation of TiO$_2$ [7].

The aqueous solution of MO (0.25 L and known concentration) was prepared with distilled water at the natural pH 6.9 and then transferred into the double envelope reactor containing the sample of immobilized TiO$_2$ films or stored in dark. The catalyst sample was located 20 mm from the bottom of the double envelope and fixed to the top of it by a stainless-steel support. The photocatalytic experiments were carried out at 23°C. The dye solution was magnetically stirred at known stirring speed ($S$) in the dark for 30 min to ensure the adsorption–desorption equilibrium of the dye solution and the catalyst films [22]. During the reaction, the concentration of the dye was monitored by measuring the absorption of the solution using the UV–visible spectrophotometer (Biochrom Lightwave II, Cambridge, UK).

## 2.4. Procedure

The photocatalytic experiments were conducted under optimum operating conditions determined in the previous study (solution pH 3, three coated layers of TiO$_2$ powder of 98.9 mg, highlight intensity ($I$) of 65.85 W/m$^2$, stirring speed ($S$) of 800 rpm). The decolorization (%) and the mineralization (%) of the azo dye were used as indicators to evaluate and compare the performance of the photocatalytic processes in the MO dye elimination.

The measurements of the dye photo-decolorization were made by checking the variation of the dye absorption during the time course of the reaction. The dye absorption was monitored on a UV–visible spectrophotometer (Biochrom Lightwave II). The maximal wavelength ($\lambda_{max}$) represents the maximum absorption band of the dye solution and it is due to the color of this solution [25]. $\lambda_{max}$ was experimentally obtained for each initial MO concentration used in the photo-decolorization test, $\lambda_{max}$ was found to be 465 and 506 nm for the solution pH 6.9 (natural pH) and pH 3 (acidic pH), respectively.

The MO decolorization efficiency (%) for the corresponding $\lambda_{max}$ was determined by using the following equation [25]:

$$\text{Decolorization}(\%) = \frac{C_0 - C}{C_0} \times 100 \qquad (1)$$

where $C_0$ is the initial concentration of MO and $C$ represents the MO concentration at time "$t$" of UV irradiation.

TOC analysis seems to be more accurate and appropriate for evaluating the decontamination of polluted waters containing organics since it takes into account all the residual carbon-containing metabolites. TOC directly evaluates the pollution level of an aqueous solution [26]. The decrease in TOC reflects the degree of mineralization [10]. The dye mineralization efficiency for the corresponding $\lambda_{max}$ was determined by means of the disappearance of TOC using the following equation:

$$\text{TOC removal}(\%) = \frac{\text{TOC}_0 - \text{TOC}}{\text{TOC}_0} \times 100 \qquad (2)$$

where $\text{TOC}_0$ is the total organic carbon of the initial concentration of dye and TOC is the total organic carbon of the dye solution at the specific time of degradation. TELEDYNE TEKMAR TOC Torch instrument from USA was used for TOC measurement.

The kinetics of photocatalytic degradation of organic compounds usually follows the Langmuir–Hinshelwood scheme [6]:

$$r = \frac{d[C]}{dt} = \frac{kKC}{1 + kKC} \qquad (3)$$

where $r$ represents the initial rate of photooxidation, $C$ the concentration of the reactant, $t$ the irradiation time, $k$ the rate constant of the reaction and $K$ is the adsorption coefficient of the reactant. At concentrations ($C \ll 1$ mM), the equation can be simplified to the apparent rate order equation [6,14]:

$$\ln\left(\frac{C_0}{C}\right) = kKt = K_{app}t \qquad (4)$$

or

$$C_t = C_0\ e^{-K_{app}t} \qquad (5)$$

where $K_{app}$ is the apparent first-order rate constant given by the slope of the graph of $\ln C_0/C$ vs. $t$ and $C_0$ is the initial concentration of the organic pollutant. Consequently, under the same condition, the initial degradation rate could be written in a form conforming to the apparent first-order rate law [6]:

$$r_0 = K_{app}C \qquad (6)$$

## 3. Results and discussion

### 3.1. Elaboration of TiO₂ films

The deposition procedure of $TiO_2$ powder is reproducible and the number of films prepared with three layers of $TiO_2$ powder shows an increasing cumulative mass of catalyst films with an increasing number of layers (one layer of 54.9 mg, two layers of 77.3 mg and three layers of 98.9 mg) [22].

### 3.2. Characterization of TiO₂ films

#### 3.2.1. Microstructure of TiO₂ films

As presented in Fig. 3. [22], the XRD patterns of immobilized $TiO_2$ films on glass showed three diffraction peaks (1, 2 and 3 layers) conform to the pure anatase phase data (JCPDS Card No. 21-1272), which has a crystalline structure with a tetragonal crystal system. It was found that the crystalline structure of catalyst was preserved in spite of several calcination in the multilayer coating process; therefore, a good photocatalytic activity is expected from the catalyst samples used. In addition, it was observed a significant increase of the intensity in XRD peaks with the increase of layers, indicating an enhanced crystallinity of the $TiO_2$ films with increasing thickness. Thus, a good photocatalytic activity is expected in the dye removal application.

#### 3.2.2. Morphology of TiO₂ films

As can be seen in Fig. 4. [22], the SEM pictures of $TiO_2$ films showed three porous structures. It was investigated by SEM that the anatase phase was mostly noticed for the three coated films. The morphology of the single coated layer

of $TiO_2$ powder showed some large microcracks due to the incomplete coating by the particles of catalyst. Since the second coating, the surfaces of the deposited films are almost recovered by small porous agglomerates of spherical particles with fewer microcracks. It's noticed that the agglomeration phenomena are caused by the spherical size of the solid $TiO_2$ particles and the like paste nature of the $TiO_2$ powder suspension in the dip-coating procedure, which promotes the formation of particle aggregate and prevents the distribution of $TiO_2$ particles on a regular coating form. It is expected a slight diminution of available surface area because of the particle aggregation. $TiO_2$ at a high concentration loading increases the degradation rate of dyes by increasing the number of $TiO_2$ particles, which increases the number of photons absorbed and the dye molecule absorbed. However, it causes the aggregation of $TiO_2$ particles, which may cause a decrease in the number of surface-active sites and an increase in the opacity and the light scattering of $TiO_2$ particles more likely to decrease the passage of radiation through the sample [22].

### 3.3. Mineralization of MO dye in UV/TiO₂ process

The mineralization of MO (0.03 mM) was investigated in two cases, under initial and optimum conditions, as shown in Fig. 5. The optimum conditions were obtained from the first study [22] in which we have studied the effect of operational parameters on the MO dye photo-decolorization. The new results of mineralization are presented with those of the decolorization [22] to show the difference between these processes. Fig. 5. shows that the optimization of operational conditions has increased the TOC and color removal from 27.4% and 39.9% to 87.39% and 98.9%, respectively, and reduced the reaction time from 300 to 60 min. The decolorization and mineralization of MO dye were much improved
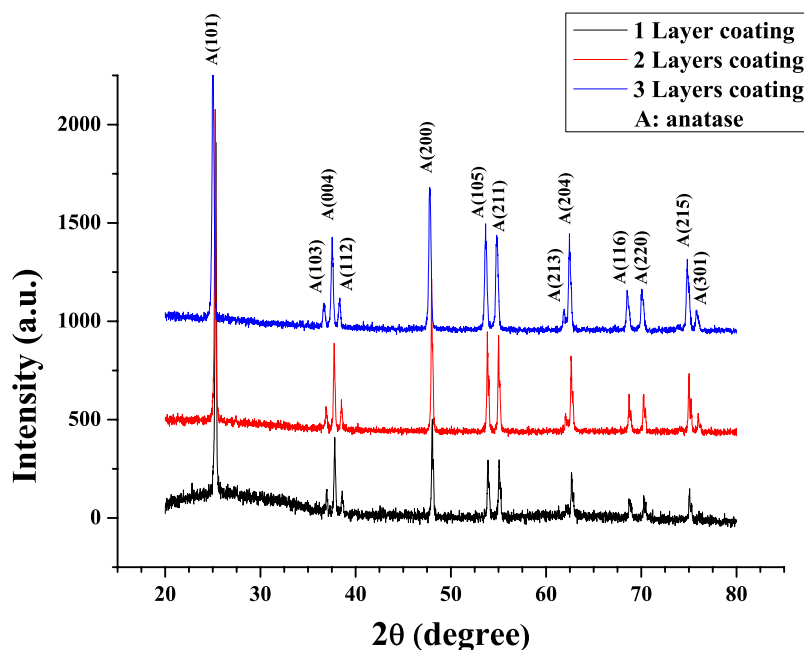


Fig. 3. X-ray diffraction patterns of $TiO_2$ films immobilized on glass by dip-coating technique. Reproduced from the Journal of Environmental Chemical Engineering [22], Copyright (2017), with permission from Elsevier.
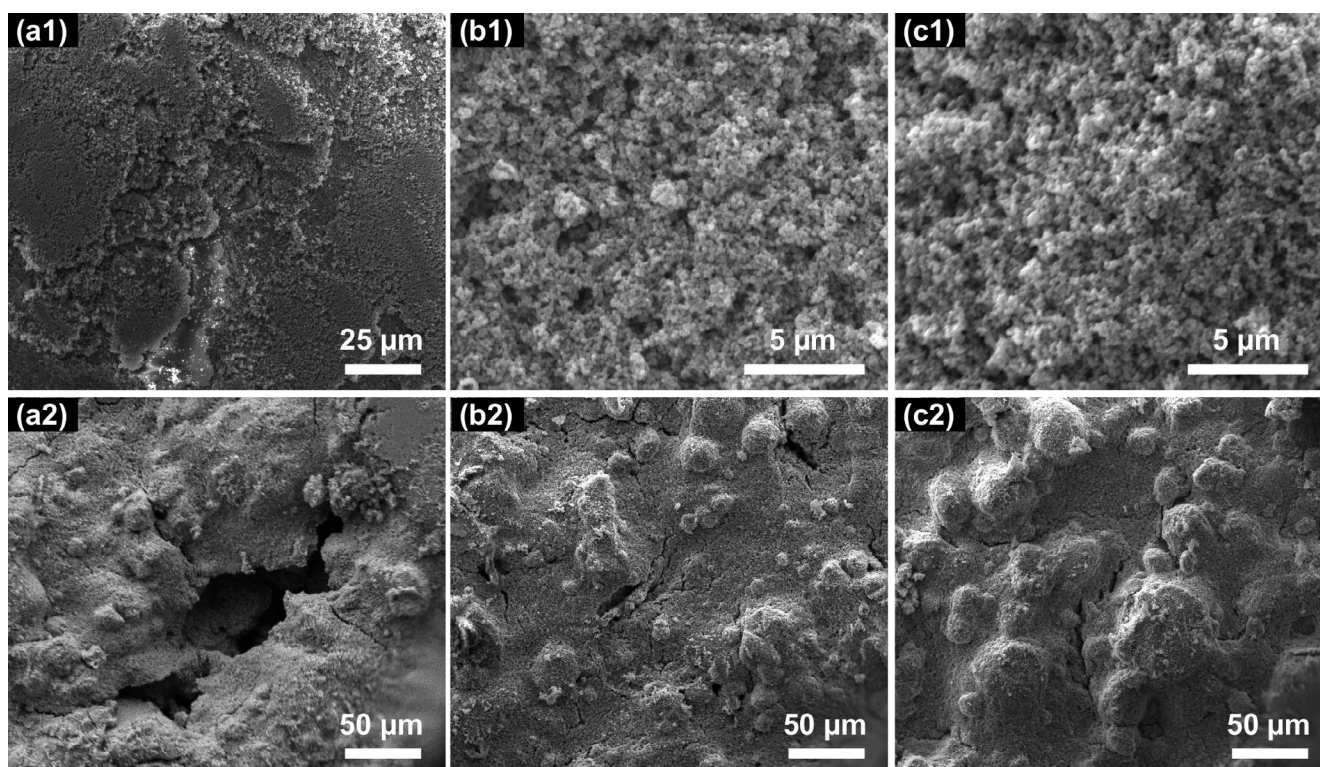
Fig. 4. SEM photographs of porous $TiO_2$ films showing the surface morphology of 1 layer (a1, a2), 2 layers (b1, b2) and 3 layers (c1, c2) immobilized by dip-coating technique. Reproduced from the Journal of Environmental Chemical Engineering [22], Copyright (2017), with permission from Elsevier.
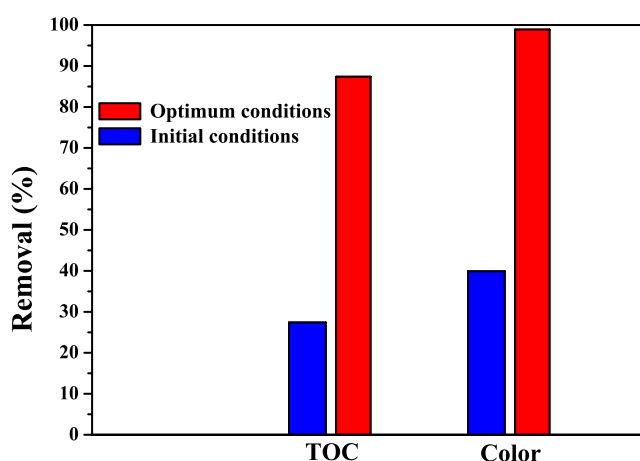


Fig. 5. Effect of operational conditions on the TOC and color removal of MO, after 60 min of irradiation in the UV/$TiO_2$ process. $[MO]_0$ = 0.03 mM; initial conditions (single layer of $TiO_2$ powder coated-glass = 54.9 mg, pH = 6.9, $I$ = 17.25 W/m², $S$ = 600 rpm); optimum conditions (three layers of $TiO_2$ powder coated-glass = 98.9 mg, pH = 3, $I$ = 65.85 W/m², $S$ = 800 rpm).

under optimum operating conditions. Thus, the optimum parameters have improved the performance of the UV/$TiO_2$ process where the photocatalytic oxidation of dye was 5 times more rapid under optimum conditions than that under initial conditions. In both latter cases, the final levels of dye

decolorization were higher than those of mineralization. Consequently, the MO mineralization was slower than the decolorization process. This slowness is due to the formation of intermediate organic products during the oxidation of the dye molecules. The same difference between the decolorization and the degradation of MO was explored by many authors. Trabelsi et al. [27] studied the solar photocatalytic decolorization and degradation of MO by the use of immobilized $TiO_2$. The authors reported that 92% decolorization and 70% mineralization of MO (0.015 g/L initial concentration) were achieved in 360 min of UV irradiation. The authors have indicated that the formation of organic intermediates by oxidation can affect TOC value in the irradiated solution and the TOC values decrease slowly because organic intermediates are deeply oxidized to $CO_2$. Another reason for the slowdown in TOC removal is the fact that the intermediate products such as carboxyl acids are more difficult to oxidize more than their parent compound (azo dye in this case). Complete oxidation proceeds at a much slower reaction rate. Ljubas et al. [28] studied the decolorization and degradation of MO dye by the use of $TiO_2$ (1,500 mg/L) nanoparticles activated by UV-A solar-like irradiation. Total decolorization of the solution and 90% TOC removal were achieved within 30 min. Compared to the decolorization process, the mineralization was slower. The authors reported that the degradation products of the dyes are certainly still present in the solution. For their total removal, the period of radiation exposure should be prolonged. A lower efficiency in the TOC content removal was expected because the developed intermediates compete

with the parent dye molecules MO during the degradation process. This finding is in agreement with the literature. The slow kinetics of dye degradation after a certain time was explained by the difficulty in converting the N-atoms of the dyes into oxidized nitrogen compounds, which implicates that the higher number of azo-groups in the dye molecule slows down the degradation process [29,30]. Thus, the necessity to totally eliminate the degradation of products formation, which is important regarding the ecotoxicity of MO azo dye and its intermediate products.

### 3.4. UV/$H_2O_2$ process

#### 3.4.1. Effect of initial dye concentration

The use of an oxidizing reagent such as $H_2O_2$ became necessary to accelerate the dye decomposition process. It has been reported that the presence of $H_2O_2$ in solutions exposed to UV irradiation of wavelength below 280 nm provokes the generation of hydroxyl radicals. OH$^\bullet$ according to the following equation [29]:

$$H_2O_2 \xrightarrow{\ hv\ <\ 280\ nm\ } 2OH^\bullet \qquad (7)$$

Therefore, it is believed that in this case, OH$^\bullet$ radicals were generated by the photolysis of $H_2O_2$ molecules and, consequently, these radicals oxidized the dye molecules leading to intermediate compounds and finally to the complete decolorization, degradation, and mineralization of the solution. Hence, the reaction rate was dramatically increased when $H_2O_2$ was added to the dye solution that was subjected to UV irradiation [29].

The effect of initial MO concentration, ranging from 0.015 to 0.06 mM, on the decolorization and mineralization efficiencies in the UV/$H_2O_2$ process was investigated. The initial dye solutions were prepared at acidic pH 3. The dosage of hydrogen peroxide added was adjusted ($[H_2O_2]_0/[MO]_0 = 500$), in order to provide sufficient hydroxyl radicals throughout the reaction [29]. Figs. 6 and 8, respectively, show the variation
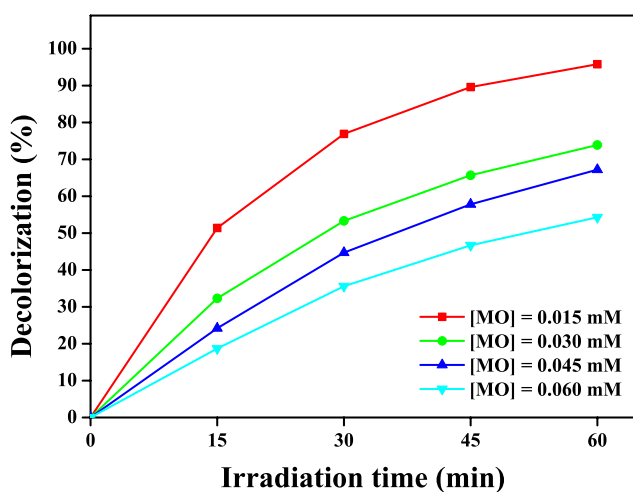
of MO decolorization and mineralization in reaction time for four initial dye concentrations studied. The final decolorization and mineralization efficiencies decreased as the initial dye concentration increased. For the initial concentrations of 0.015, 0.03, 0.045, and 0.06 mM, 95.8%, 73.9%, 67.2%, and 54.3% MO decolorization, respectively, and 83.77%, 61.93%, 55.20%, and 42.13% MO mineralization, respectively, were achieved after 60 min of UV irradiation. It is observed that for all initial dye concentrations studied, the mineralization of MO was slower than its decolorization.

From the data in Fig. 7, it can be observed that the decolorization reaction kinetic can be considered first order for all initial concentrations studied. The rate constants obtained were confirmed the decolorization efficiencies obtained in Fig. 6. The highest rate constant (0.0514 min$^{-1}$) was obtained for the lowest initial concentration (0.015 mM). It represented
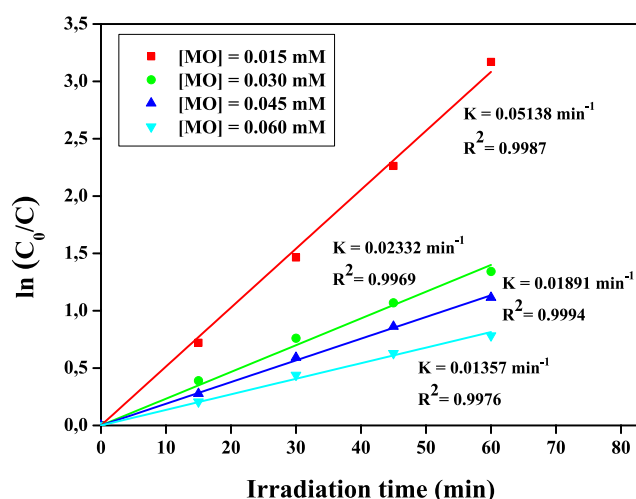


Fig. 7. First-order kinetics of MO decolorization in the UV/$H_2O_2$ process for different MO initial concentrations. MO solution pH 3, $[H_2O_2]_0/[MO]_0 = 500$, $I = 65.85$ W/m$^2$, $S = 800$ rpm.



Fig. 6. Effect of initial MO concentration on the decolorization efficiency, during 60 min of irradiation in the UV/$H_2O_2$ process. MO solution pH 3, $[H_2O_2]_0/[MO]_0 = 500$, $I = 65.85$ W/m$^2$, $S = 800$ rpm.
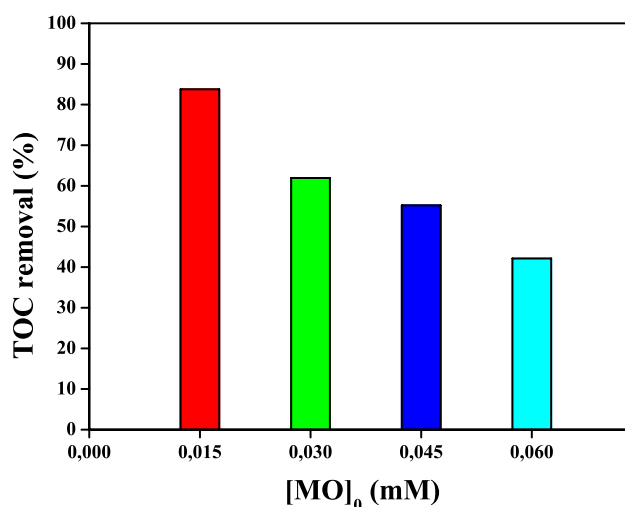


Fig. 8. Effect of initial MO concentration on the TOC removal efficiency, during 60 min of irradiation in the UV/$H_2O_2$ process. MO solution pH = 3, $[H_2O_2]_0/[MO]_0 = 500$, $I = 65.85$ W/m$^2$, $S = 800$ rpm.

the most rapid kinetic compared to others values (0.0233, 0.0189 and 0.0136 min⁻¹) for 0.03, 0.045 and 0.06 mM of the dye, respectively.

The progress of the oxidation reaction of organic molecules in the aqueous solution depends on the number of hydroxyl radicals produced by the photolysis of $H_2O_2$ and consumed by this solution. When the concentration of $H_2O_2$ is constant, the high dosage of pollutant consumes more hydroxyl radicals where their production is constant. Furthermore, at high dye concentration, a great number of molecules are present in the dye solution, which reduces both the absorption of photons and the production of highly active OH$^\bullet$ radicals and their interactions with the dye molecules in solution. For these reasons, the photooxidation of MO dye was slow in the presence of a high dosage of pollutants. Consequently, the increase in initial dye concentration has decreased the MO decolorization and mineralization.

Many published articles supported the negative effect of increasing dye concentration. Haji et al. [24] studied the effect of MO initial concentration ranging from $1.46 \times 10^{-5}$ to $9.27 \times 10^{-5}$ mol/L on the dye degradation when MO was treated by UV/$H_2O_2$ with keeping $[H_2O_2]_0$ constant at $4.58 \times 10^{-2}$ mol/L. The authors indicated that the time required to achieve a specific conversion increases as the initial dye concentration increases as well. It was reported that the behavior of slow dye elimination with increasing dosage of MO dye was found reasonable because as the dye concentration increased, the solution became less permeable to UV irradiation. Consequently, the UV irradiation received by $H_2O_2$ molecules decreased, leading to a decrease in the generated hydroxyl radicals' concentration. Seyedsalehi et al. [30] have found that the color removal efficiency of acid orange 7 colors was reduced from 72% to 63% when the initial concentration of the dye was increased from 25 to 75 mg/L. The authors have indicated that in the advanced oxidation system based $H_2O_2$, since, hydroxyl radical production remains constant under constant operational conditions, therefore, by increasing the concentration of pollutants, the radicals will be consumed and consequently the efficiency of the process will be decreased. Manikandan et al. [31] evaluated the UV/$H_2O_2$ process for the degradation of orange acid 7. The authors reported that the dye degradation efficiency decreased with the increase of its initial concentration (100–500 mg/L). They indicated that high dye concentration could be unfavorable to the UV light penetration and thus decreases the reaction rate. Also, two published works have reported the same reason for that behavior [32,33]. The papers were agreed on the fact that at high dye concentration, the penetration of photons entering into the solution decreases and hence the solution became more and more impermeable to the UV irradiation which causes a reduction in hydroxyl radical concentration. Consequently, the dyes' photo-oxidation efficiency decreases.

### 3.4.2. Effect of initial $H_2O_2$ concentration

In the objective of investigating the effect of hydrogen peroxide concentration on the decolorization and mineralization efficiencies of the dye, five different dosages of $H_2O_2$ (10.57, 17.60, 24.63, 35.14 and 43.88 mM) were added to MO initial concentration (0.03 mM, pH 3). The experiments were conducted in the same optimum photocatalytic

reactor used in UV/$TiO_2$ process. Figs. 9 and 10 show that as $[H_2O_2]_0$ increased from 10.57 to 17.60 mM, the dye decolorization and mineralization efficiencies were slightly increased from 94.1% and 82.71% to 99.8% and 87.79%, respectively, in 60 min of UV irradiation. However, when $[H_2O_2]_0$ was further increased beyond 17.60 mM, the decolorization and mineralization efficiencies were decreased after each step of increasing $[H_2O_2]_0$ up to 43.88 mM in which the decolorization and mineralization efficiencies obtained, respectively, were 90.3% and 78.41%, 86.2% and 74.32%, 81.5%, and 68.95%, for 24.63, 35.14 and 43.88 mM of $[H_2O_2]_0$, respectively.

In the present study, the optimum $[H_2O_2]_0$ that has led to high dye decolorization and mineralization, was found to be 17.60 mM which corresponding to a $[H_2O_2]_0/[MO]_0$ molar ratio of 587. Many authors confirmed that an optimum of $[H_2O_2]_0$ existed for getting high dyes decolorization
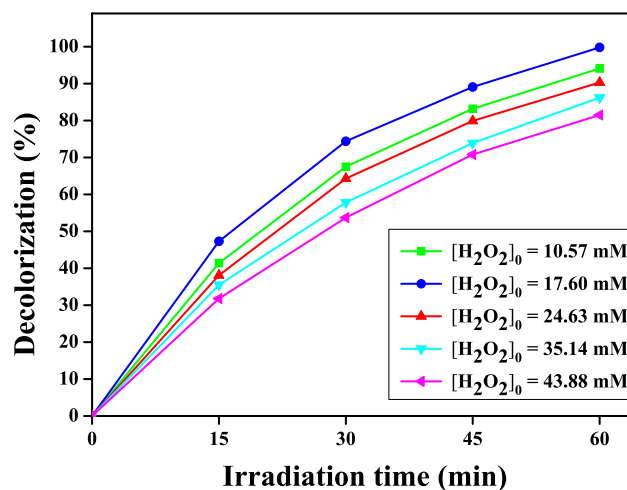
Fig. 9. Effect of initial $H_2O_2$ concentration on the MO decolorization, during 60 min of irradiation in the UV/$H_2O_2$ process. $[MO]_0$ = (0.03 mM, pH 3), $I$ = 65.85 W/m², $S$ = 800 rpm.
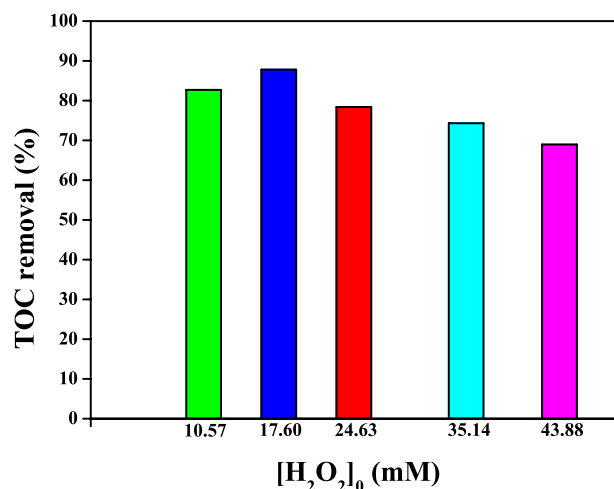
Fig. 10. Effect of initial $H_2O_2$ concentration on the TOC removal of MO, during 60 min of irradiation in the UV/$H_2O_2$ process. $[MO]_0$ = (0.03 mM, pH 3), $I$ = 65.85 W/m², $S$ = 800 rpm.

and degradation. Haji et al. [24] have found a $[H_2O_2]_0/[MO]_0$ molar ratio of 590 for the degradation of MO by UV/$H_2O_2$ process. Shu et al [29] reported that the optimum ratio of $[H_2O_2]_0/[dye]_0$ for the decolorization of Acid Black 1 by UV/$H_2O_2$ process was from 500 to 800. Initially, the increase of $[H_2O_2]_0$ has increased the production of hydroxyl radicals, according to reaction (7) and, therefore, the initial dye decolorization increased. However, a further increase of $[H_2O_2]_0$ promoted the production of hydroperoxyl radicals according to the following reaction [34]:

$$OH^\bullet + H_2O_2 \rightarrow H_2O + HO_2^\bullet \qquad (8)$$

Hydroperoxyl radicals ($HO_2^\bullet$) are of less oxidizing power than the hydroxyl radicals ($OH^\bullet$). Therefore, the excess of $H_2O_2$ molecules consumed the highly active hydroxyl radicals and, consequently, reduced the rate of the dye elimination reaction [23]. Vaez et al. [35] reported on the existence of an optimum value of $[H_2O_2]_0$ which leads to significant levels of dye decolorization and degradation. They indicated that hydrogen peroxide can increase the formation rate of hydroxyl radicals in two ways. First, the reduction reaction of $H_2O_2$ at the conduction band would produce hydroxyl radicals. Second, the self-decomposition by irradiation would also produce hydroxyl radicals. Bouanimba et al [36] have found that the decolorization of BPB was enhanced by the addition of low $H_2O_2$ dosage and retarded while overdose was used, due to the formation of less reactive hydroperoxyl radicals.

As an important remark from the data of the UV/$H_2O_2$ photooxidation process, the dye mineralization was slower than the decolorization process. The same behavior was found by Zuorro et al., where they studied the degradation of diazo dye Reactive Green 19 in aqueous solution ($6.34 \times 10^{-5}$ M) by UV/$H_2O_2$ AOP [37]. Under optimum pH and $H_2O_2$ dose, 100% of color removal and 63% of TOC removal were achieved after 20 and 90 min of UV irradiation, respectively.

### 3.5. TiO$_2$/UV/H$_2$O$_2$ system

Reports showed that oxidizing agents have a great deal of influence on the photocatalytic decolorization, degradation and mineralization of dyes [34].

In UV/TiO$_2$ process, after a slower process of only 39.9% dye color removal and 27.40% TOC removal achieved in 300 min under initial conditions, 98.9% dye color removal and 87.39% TOC removal were achieved in 60 min under optimized conditions. The optimization of operational parameters has improved the MO decolorization and mineralization by UV/TiO$_2$ process. Despite this good result, the elimination of MO by the use of UV/ TiO$_2$ process alone still needed more improvement to reach rapid practical wastewater decontamination under UV light irradiation.

It is expected that the addition of $H_2O_2$ will produce an electron acceptor and accelerate MO removal. Thus, to make the MO elimination much faster and testing the effect of electron acceptor on the UV/TiO$_2$ process under optimum operating parameters, experiments were conducted at different concentrations of $H_2O_2$ ranging from 5.29 to 17.6 mM with maintaining the amount of catalyst at 98.9 mg and the dye concentrations at 0.03 mM.

From the data in Figs. 11 and 13, when 5.29 mM $H_2O_2$ was added to the dye solution in the presence of three coated layers of TiO$_2$ powder, the decolorization and mineralization of MO reached 90.22% and 79.21%, respectively, within only 10 min of reaction. The photocatalyst sample used with the addition of 10.57 mM $H_2O_2$ exhibited the highest photocatalytic activity in MO elimination (100% decolorization and 88.99% mineralization achieved within only 10 min of reaction). In the UV/TiO$_2$ process, 98.9% decolorization and 87.39% mineralization of MO were achieved in 60 min. Thus, TiO$_2$/UV/H$_2$O$_2$ Process was more efficient and 6 times more rapid than UV/TiO$_2$ process. This is attributable to the $H_2O_2$ facilitating the generation of hydroxyl radicals, which are powerful oxidizing agents to effectively promote the photo-decolorization and the photo-mineralization of MO [38]. However, further, an increase in $H_2O_2$ dosage added beyond 10.57 mM impeded the MO elimination resulting in the decolorization and mineralization efficiencies of 93.9% and 82.89%, 86.7% and 75.69%, respectively, for 14.09 and 17.6 mM $H_2O_2$, respectively.

The rate constants obtained in Fig. 12 were followed the same behavior as the decolorization efficiencies obtained in Fig. 11. The Highest rate constant (0.2834 min$^{-1}$) was obtained for the optimum $H_2O_2$ initial concentration (10.57 mM) which represented the most rapid kinetic compared to others values (0.2259, 0.1884 and 0.1697 min$^{-1}$) for 14.09, 5.29 and 17.6 mM $H_2O_2$, respectively. It can be concluded that the addition of $H_2O_2$ with an optimal concentration of 10.57 mM has strongly enhanced photo-decolorization and photo-mineralization and reduced the time needed for complete MO elimination. However, the addition of $H_2O_2$ beyond the optimal value has reduced the dye elimination efficiency.

Many published papers have justified similar findings. Niu and Hao [15] studied the effect of $H_2O_2$ addition on the dye photooxidation efficiency. The authors indicated that the enhanced degradation effect should be attributed to the increase of electron–hole separation efficiency and the concentration of hydroxyl radicals ($OH^\bullet$) generated through the
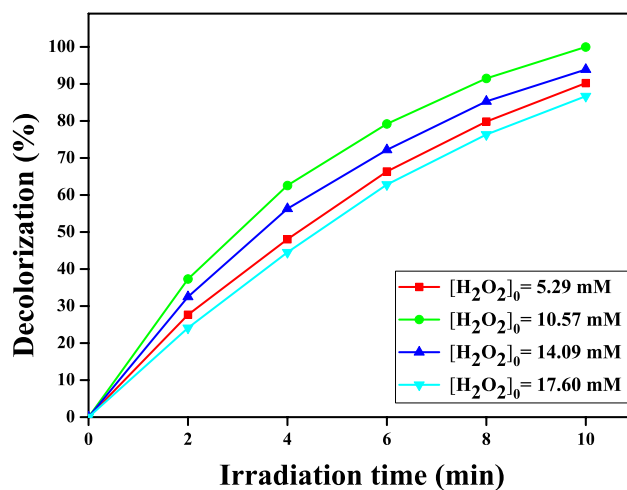


Fig. 11. Effect of $H_2O_2$ initial concentration on the MO decolorization, during 10 min of irradiation in the TiO$_2$/UV/H$_2$O$_2$ process. Three layers of TiO$_2$ powder coated-glass = 98.9 mg, $[MO]_0$ = (0.03 mM, pH 3), $I$ = 65.85 W/m$^2$, $S$ = 800 rpm.
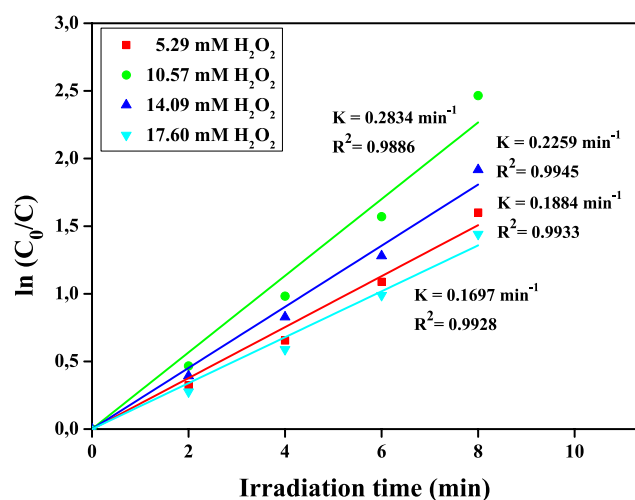
Fig. 12. First-order kinetics of MO decolorization in the $TiO_2$/UV/$H_2O_2$ process for different $H_2O_2$ initial concentrations. Three layers of $TiO_2$ powder coated-glass = 98.9 mg, $[MO]_0$ = (0.03 mM, pH 3), $I$ = 65.85 W/m², $S$ = 800 rpm.
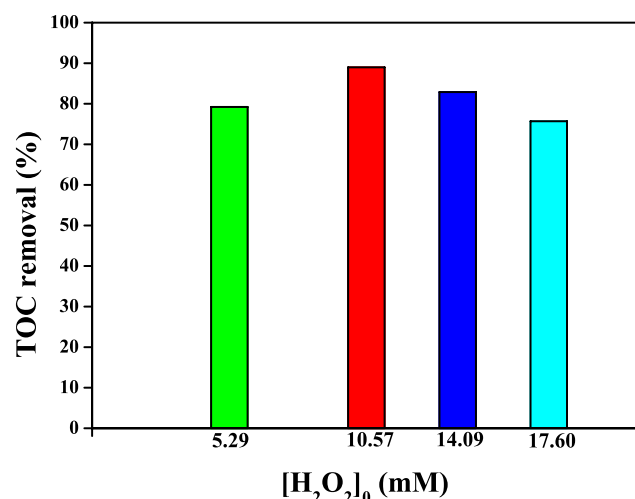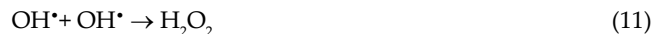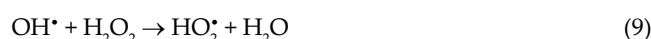


Fig. 13. Effect of $H_2O_2$ initial concentration on the TOC removal of MO, during 10 min of irradiation in $TiO_2$/UV/$H_2O_2$ process. Three layers of $TiO_2$ powder coated-glass = 98.9 mg, $[MO]_0$ = (0.03 mM, pH 3), $I$ = 65.85 W/m², $S$ = 800 rpm.

reactions of $H_2O_2$ with the photogenerated electrons or the direct photolysis of $H_2O_2$. The addition of irreversible electron acceptor $H_2O_2$ captures the conduction band electron and promotes the electron–hole separation. This means that the available number and the survival time of holes can be increased and higher degradation percentage is obtained in a relatively short time. In addition, hydroxyl radical (OH•) produced is a strong oxidant and plays a dominant role in the photocatalytic process of some dyes. Therefore, the increase in the concentration of hydroxyl radicals (OH•) will facilitate the fast decolorization and degradation of MO [15].

Many other authors have studied the effect of $H_2O_2$ addition on the photocatalytic elimination of dyes. Ouyang et al [38] reported on the MO decolorization by MWCNTs/
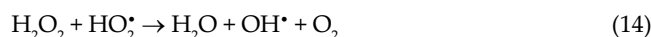
$TiO_2$/CdS composite. With 4 mmol/L $H_2O_2$ added, the decolorization of MO reached about 94.4% within 80 min. The sample treated with the addition of optimum $H_2O_2$ (10 mmol/L) exhibited the highest photocatalytic activity; the decolorization of MO reached about 98.3% within 80 min. Interestingly, a further increase of the $H_2O_2$ concentration to 30 mmol/L impeded the decolorization of MO (72.4% after 80 min of irradiation). Huang et al. [16] reported for the photocatalytic decolorization of MO solution by Pt modified $TiO_2$ loaded on the natural zeolite, an optimum addition of 1.2 mM/L $H_2O_2$ appeared when the concentration of $H_2O_2$ ranged from 0.4 to 2 mM/L. Zhiyong et al. [12] reported that the solution was discolored in 1 h by the addition of 1 mM $H_2O_2$ to the sunlight irradiated $TiO_2$ P25 suspension (0.5 g/L). Akpan and Hameed [8] revealed the effect of oxidants on the photocatalytic reactions. The decolorization and degradation efficiencies of dyes on $TiO_2$ photocatalyst attained the maximum at the optimum $H_2O_2$ dosage. At a higher dosage of $H_2O_2$ beyond the optimum, the decolorization and degradation efficiencies of dyes decreased. This was because the highly reactive OH• radicals could be consumed by the $H_2O_2$ itself as given in Eqs. (9) and (10) [10]. At the same time, radical–radical recombination as a competitive reaction must be taken into account, as described in Eq. (11) [10].

$$OH^• + H_2O_2 \rightarrow HO_2^• + H_2O \tag{9}$$

$$OH^• + HO_2^• \rightarrow O_2 + H_2O \tag{10}$$

$$OH^• + OH^• \rightarrow H_2O_2 \tag{11}$$

As OH• radicals are strong oxidants for organic pollutants, the photocatalytic decolorization and degradation of dyes will be inhibited in the condition of an excess of $H_2O_2$. Furthermore, $H_2O_2$ can be adsorbed onto $TiO_2$ particles to modify their surfaces and subsequently decreased its photocatalytic activity [8].

In addition, Andronic et al. [23] explained the influence of $H_2O_2$ on the $TiO_2$-based system by the role of $H_2O_2$ in generating the reactive species as expressed in the following scheme:

### 3.5.1. OH• generation

$$H_2O_2 + h\nu \rightarrow 2OH^• \tag{12}$$

$$H_2O_2 + OH^• \rightarrow H_2O + HO_2^• \tag{13}$$

$$H_2O_2 + HO_2^• \rightarrow H_2O + OH^• + O_2 \tag{14}$$

### 3.5.2. Inhibition of the electron–hole recombination

$$H_2O_2 + e^- \rightarrow OH^• + OH^- \tag{15}$$

$$H_2O_2 + 2h_{VB}^+ \rightarrow O_2 + 2H^+ \tag{16}$$

$$H_2O_2 + h_{VB}^+ \rightarrow HO_2^• + H^+ \tag{17}$$

*3.5.3. Photodecolorization and photo-mineralization of dye*

$$HO_2^\bullet, OH^\bullet + \text{organic dye} \rightarrow \text{intermediates} \rightarrow$$
$$CO_2 + H_2O + \text{inorganic compounds} \quad (18)$$
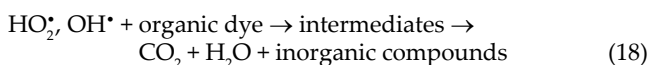
In these mechanisms, the $O_2$ and the $H_2O_2$ containing systems produced active species ($OH^\bullet$) and generated different species characterizing the $O_2$ containing system ($^-O–O^\bullet$) and the $H_2O_2$ system ($HO_2^\bullet$). Their different activities can induce different dye photo-elimination by-products or interims. These unstable species leading to different reaction rates and efficiencies [23].

Another remark that was observed in this experiment is that in all TOC removal processes, the mineralization process was slower than the decolorization resulting in final percentages of TOC removal lower than final decolorization percentages. Thus, more time of mineralization is needed to achieve the same specific decolorization progress. The reason for this slowness is that as the initial concentrations of the dyes increase, the formation of organic intermediate species increases as well and therefore, the effectiveness of the mineralization decreases. Many authors supported this slowness and explained its reasons. Tseng et al. [39] studied the influence of hydrogen peroxide on the degradation and mineralization of monochlorobenzene (MCB) during UV/$TiO_2$ process. The experiments revealed that the complete destruction of MCB was observed within 120 min of irradiation in the presence of $TiO_2$ catalyst and the optimum $H_2O_2$ dosage. However, the mineralization efficiency was about 87.4% after 240 min of illumination time. The authors indicated that the TOC decayed with illumination time in parallel with the MCB degradation. However, it should be noted that the complete disappearance of MCB occurred within 120 min of irradiation under various initial concentrations of the electron acceptor, whereas residual TOC was still observed. This phenomenon implied that transient organic intermediates were likely to present in the photocatalytic system. Kulkarni and Thakur [19] reported that complete decolorization and 65% substantial mineralization of Navy blue HE2R 1 azo dye (0.025 mmol/L) was achieved in 1 h by UV/$TiO_2$/ZnO/$H_2O_2$ process with an optimum $[H_2O_2]_0$ of 0.375 g/250 mL. The authors indicated that the reduction in TOC values of the treated dye solution indicates the mineralization of dye molecules along with color removal. Zhang et al. [10] reported that the TOC removal time was obviously longer than decolorization time in the methylene blue oxidation process. The authors stated that the dye molecules are decomposed to lower molecular weight compounds and the intermediates still contribute to the TOC of the dye solution. The emergence of mineralization plateau indicates that the total oxidation is nearing completion, corresponding to the oxidation of most stable products. Yaman and Gündüz [40] studied the decolorization and mineralization of C.I. Reactive Red 141 in water by a heterogeneous oxidation process. They reported that the decolorization of the diazo reactive textile dye is a result of N=N bond destruction with the addition of $OH^\bullet$ radicals. The mineralization of dye is the total oxidation of the intermediate products to $CO_2$ and $H_2O$ and it is slower than color removal because of the priority of the attack of $OH^\bullet$ on the N=N bonds of the azo dye. The same reason is admitted in the case of the MO azo compound which contains N=N bond in its molecular structure. Hence, that priority has favored the color removal process compared to the difficulty of attacking the aromatic part in the dye molecules and has delayed the total mineralization of the azo dye compound.

*3.6. Comparison of UV/$TiO_2$, UV/$H_2O_2$ and $TiO_2$/UV/$H_2O_2$ processes*

UV/$TiO_2$, UV/$H_2O_2$ and $TiO_2$/UV/$H_2O_2$ were applied under optimum operating conditions. The reaction time and the final levels of the MO decolorization and mineralization achieved by each process determine its rapidity and efficiency. For comparison, the optimum UV/$TiO_2$ process has improved the MO elimination by enhancing the decolorization and mineralization from 39.9% and 27.4% to 98.9% and 87.39%, respectively and reducing the reaction time from 5h to 1 h. The use of UV/$H_2O_2$ at a critical initial concentration of $H_2O_2$ (17.60 mM) produced 99.8% decolorization and 87.79% mineralization in only 1 h of UV irradiation. Significantly, in the optimum reactor, both UV/$TiO_2$ and UV/$H_2O_2$, processes are capable to deliver almost the same MO elimination levels within the same period of time. Autin et al [7] studied the degradation of 1 mg/L metaldehyde by 1.2 mg/L $TiO_2$ or 8 mM $H_2O_2$, the photodegradation kinetic rate revealed almost similar value for both UV/$TiO_2$ and UV/$H_2O_2$ indicating that both processes are capable to deliver the same levels of dye photooxidation.

Until now the high levels of dye decolorization and mineralization obtained by both UV/$TiO_2$ and UV/$H_2O_2$ processes still needed more advance to make the reaction time more rapid for complete MO elimination. To achieve this objective, a combination of immobilized photocatalyst with the oxidizing agent was conducted.

In the presence of 10.57 mM $H_2O_2$ and 98.9 mg of fixed $TiO_2$, 100% dye color removal and 88.99% TOC removal were achieved in just 10 min of reaction. The photocatalytic oxidation of MO (0.03 mM) by the use of $TiO_2$/UV/$H_2O_2$ system was found to be much more rapid than either UV/$TiO_2$ or UV/$H_2O_2$ alone. Similarly published works supported these findings. Niu and Hao [15] reported that in the photocatalytic degradation of MO (20 mg/L) conducted at different concentrations of $H_2O_2$ ranges from 2.5 to 20 mM, more than 96.00% of MO was decolorized within 30 min in the presence of 20 mM $H_2O_2$, instead of 84.09% color removal within 60 min in the absence of $H_2O_2$.

**4. Conclusions**

In summary, the present work improved the performance of UV/$TiO_2$, UV/$H_2O_2$ and $TiO_2$/UV/$H_2O_2$ systems for the mineralization and decolorization of MO azo dye pollutant via the synergistic effect of optimum conditions. In the optimum reactor, the UV/$TiO_2$ process has effectively decolorized 98.9% and mineralized 87.39% of MO in 60 min of UV irradiation. The photocatalytic oxidation of MO azo dye by UV/$TiO_2$ system was 5 times more rapid under optimum conditions than that under initial conditions. UV/$H_2O_2$ has efficiently removed the pollution of MO aqueous solution (99.8% decolorization and 87.79% mineralization) at a critical concentration of 17.60 mM (corresponding to a $[H_2O_2]_0/[MO]_0$

molar ratio of 587) in 60 min of reaction. In the presence of three coated layers of TiO$_2$ photocatalyst (98.9 mg) and 10.57 mM [H$_2$O$_2$]$_0$ (corresponding to a [H$_2$O$_2$]$_0$/[MO]$_0$ molar ratio of 352), total dye color removal and 88.99% dye mineralization were achieved with rapid oxidation kinetic of just 10 min. This synergistic advancement thereby allowing to accelerate 6 times the elimination of MO azo dye is attributed to the combination between the immobilized layers of highly active TiO$_2$ catalyst and the optimum H$_2$O$_2$ oxidizing agent. This synergy ability for promoting the generation of both powerful oxidants (OH$^•$ hydroxyl radicals in priority) and photoexcited electron-hole pairs.

It has been demonstrated that at low pollutant concentrations ($C \ll 1$ mM), the kinetics of heterogeneous reaction fitted the first-order model of Langmuir–Hinshelwood. This study has well supported this fact. In addition, the nature of organic pollutants and their by-products has slowed down the mineralization process. This study has developed a photocatalytic system for high-performance based on immobilized TiO$_2$ layers and optimum H$_2$O$_2$ dosage. However, the identification of organic intermediate products is essential to further accelerate the destruction of organic pollutants in water and should be the primary focus in future similar environmental researches.

## References

[1] I. Oller, S. Malato, J.A. Sánchez-Pérez, Combination of advanced oxidation processes and biological treatments for wastewater decontamination–a review, Sci. Total Environ., 409 (2011) 4141–4166.

[2] O. Tokode, R. Prabhu, L.A. Lawton, P.K.J. Robertson, Controlled periodic illumination in semiconductor photocatalysis, J. Photochem. Photobiol., A., 319–320 (2016) 96–106.

[3] M.C. Chang, H.Y. Shu, T.H. Tseng, H.W. Hsu, Supported zinc oxide photocatalyst for decolorization and mineralization of orange G dye wastewater under UV365 irradiation, Int. J. Photoenergy, 2013 (2013) 1–12, https://doi.org/10.1155/2013/595031.

[4] S. Krishnan, H. Rawindran, C.M. Sinnathambi, J.W. Lim, Comparison of various advanced oxidation processes used in remediation of industrial wastewater laden with recalcitrant pollutants, Mater. Sci. Eng., 206 (2017) 1–11.

[5] H. Huang, D.Y.C. Leung, P.C.W. Kwong, J. Xiong, L. Zhang, Enhanced photocatalytic degradation of methylene blue under vacuum ultraviolet irradiation, Catal. Today, 201 (2013) 189–194.

[6] U.I. Gaya, A.H. Abdullah, Heterogeneous photocatalytic degradation of organic contaminants over titanium dioxide: a review of fundamentals, progress and problems, J. Photochem. Photobiol., C, 9 (2008) 1–12.

[7] O. Autin, J. Hart, P. Jarvis, J. MacAdam, S.A. Parsons, B. Jefferson, Comparison of UV/H$_2$O$_2$ and UV/TiO$_2$ for the degradation of metaldehyde: kinetics and the impact of background organics, Water Res., 46 (2012) 5655–5662.

[8] U.G. Akpan, B.H. Hameed, Parameters affecting the photocatalytic degradation of dyes using TiO$_2$-based photocatalysts: a review, J. Hazard. Mater., 170 (2009) 520–529.

[9] N.M. Mahmoodi, M. Arami, N.Y. Limaee, N.S. Tabrizi, Decolorization and aromatic ring degradation kinetic of direct red 80 by UV oxidation in the presence of hydrogen peroxide utilizing TiO$_2$ as a photocatalyst, Chem. Eng. J., 112 (2005) 191–196.

[10] Q. Zhang, C. Li, T. Li, Rapid photocatalytic decolorization of methylene blue using high photo flux UV/TiO$_2$/H$_2$O$_2$ process, Chem. Eng. J., 217 (2013) 407–413.

[11] S. Kang, L. Zhang, C. Liu, L. Huang, H. Shi, L. Cui, Hydrogen peroxide activated commercial P25 TiO$_2$ as efficient visible-light-driven photocatalyst on dye degradation, Int. J. Electrochem. Sci., 12 (2017) 5284–5293.

[12] Y. Zhiyong, H. Keppner, D. Laub, E. Mielczarski, J. Mielczarski, L. Kiwi-Minsker, A. Renken, J. Kiwi, Photocatalytic discoloration of Methyl Orange on innovative parylene –TiO$_2$ flexible thin films under simulated sunlight, Appl. Catal., B, 79 (2008) 63–71.

[13] T.A. Egerton, H. Purnama, Does hydrogen peroxide really accelerate TiO$_2$ UV-C photocatalyzed decolorization of azo-dyes such as Reactive Orange 16?, Dyes Pigm., 101 (2014) 280–285.

[14] Z. Hua-yue, J. Ru, G. Yu-jiang, F. Yong-qian, X. Ling, Z. Guang-ming, Effect of key operational factors on decolorization of methyl orange during H$_2$O$_2$ assisted CdS/TiO$_2$/ploymer nanocomposite thin films under simulated solar light irradiation, Sep. Purif. Technol., 74 (2010) 187–194.

[15] P. Niu, J. Hao, Photocatalytic degradation of methyl orange by titanium dioxide-decatungstate nanocomposite films supported on glass slides, Colloids surf., A, 431 (2013) 127–132.

[16] M. Huang, C. Xu, Z. Wu, Y. Huang, J. Lin, J. Wu, Photocatalytic discoloration of methyl orange solution by Pt modified TiO$_2$ loaded on natural zeolite, Dyes Pigm., 77 (2008) 327–334.

[17] D. Rajamanickam, M. Shanthi, Photocatalytic degradation of an organic pollutant by zinc oxide–solar process, Arabian J. Chem., 9 (2016) S1858–S1868.

[18] Q. Zhang, C. Li, T. Li, Rapid photocatalytic degradation of Methylene Blue under high photon flux UV irradiation: characteristics and comparison with routine low photon flux, Int. J. Photoenergy, 2012 (2012) 1–7, https://doi.org/10.1155/2012/398787.

[19] M. Kulkarni, P. Thakur, Photocatalytic degradation and mineralization of reactive textile azo dye using semiconductor metal oxide nanoparticles, Int. J. Eng. Res. Gen. Sci., 2 (2014) 245–254.

[20] P. Dharmarajan, A. Sabastiyan, M. Yosuva Suvaikin, S. Titus, C. Muthukumar, Photocatalytic degradation of reactive dyes in effluents employing copper doped titanium dioxide nanocrystals and direct sunlight, Chem. Sci. Trans., 2 (2013) 1450–1458.

[21] K. Soutsas, V. Karayannis, I. Poulios, A. Riga, K. Ntampegliotis, X. Spiliotis, G. Papapolymerou, Decolorization and degradation of reactive azo dyes via heterogeneous photocatalytic processes, Desalination, 250 (2010) 345–350.

[22] A. Bouarioua, M. Zerdaoui, Photocatalytic activities of TiO$_2$ layers immobilized on glass substrates by dip-coating technique toward the decolorization of methyl orange as a model organic pollutant, J. Environ. Chem. Eng., 5 (2017) 1565–1574.

[23] L. Andronic, S. Manolache, A. Duta, Photocatalytic degradation of methyl orange: influence of H$_2$O$_2$ in the TiO$_2$-based system, J. Nanosci. Nanotechnol., 8 (2008) 728–732.

[24] S. Haji, B. Benstaali, N. Al-Bastaki, Degradation of methyl orange by UV/H$_2$O$_2$ advanced oxidation process, Chem. Eng. J., 168 (2011) 134–139.

[25] M.A. Barakat, J.M. Tseng, C.P. Huang, Hydrogen peroxide-assisted photocatalytic oxidation of phenolic compounds, Appl. Catal., B, 59 (2005) 99–104.

[26] M. Kulkarni, P. Thakur, Photocatalytic degradation of real textile industrial effluent under UV light catalyzed by metal oxide nanoparticles, Nepal J. Sci. Technol., 15 (2014) 105–110.

[27] H. Trabelsi, G.P. Atheba, O. Hentati, Y.D. Mariette, D. Robert, P. Drogui, M. Ksibi, Solar photocatalytic decolorization and degradation of methyl orange using supported TiO$_2$, J. Adv. Oxid. Technol., 19 (2016) 79–84.

[28] D. Ljubas, G. Smoljanic, H. Juretic, Degradation of methyl orange and congo red dyes by using TiO$_2$ nanoparticles activated by the solar and the solar-like radiation, J. Environ. Manage., 161 (2015) 83–91.

[29] H.Y. Shu, M.C. Chang, H.J. Fan, Decolorization of azo dye acid black 1 by the UV/H$_2$O$_2$ process and optimization of operating parameters, J. Hazard. Mater., B113 (2004) 201–208.

[30] M. Seyedsalehi, S. Mousavian, S. Eslamian, M.H. Shahmoradi, Removal efficiency of (AO7) Acid Orange 7 color using the advanced oxidation of modified UV/H$_2$O$_2$ with zero-valent iron, Bull. Environ. Pharmacol. Life Sci., 4 (2015) 140–149.

[31] P. Manikandan, P.N. Palanisamy, R. Ramya, D. Nalini, Evaluation of UV/H$_2$O$_2$ advanced oxidation process (AOP) for the degradation of acid orange7 and basic violet 14 dye in aqueous solution, Int. J. Emerging Technol. Comput. Appl. Sci., 9 (2014) 148–151.

[32] N. Daneshvar, M.A. Behnajady, M. Khayyat Ali Mohammadi, M.S. Seyed Dorraji, UV/H$_2$O$_2$ treatment of Rhodamine B in aqueous solution: influence of operational parameters and kinetic modeling, Desalination, 230 (2008) 16–26.

[33] E. Basturk, M. Karatas, Decolorization of antraquinone dye Reactive Blue 181 solution by UV/H$_2$O$_2$ process, J. Photochem. Photobiol., 299 (2015) 67–72.

[34] H. Zangeneh, A.A.L. Zinatizadeha, M. Habibi, M. Akia, M. Hasnain Isa, Photocatalytic oxidation of organic dyes and pollutants in wastewater using different modified titanium dioxides: a comparative review, J. Ind. Eng. Chem., 26 (2015) 1–36.

[35] M. Vaez, A.Z. Moghaddam, N.M. Mahmoodi, S. Alijani, Decolorization and degradation of acid dye with immobilized titania nanoparticles, Process Saf. Environ. Prot., 90 (2012) 56–64.

[36] N. Bouanimba, R. Zouaghi, N. Laid, T. Sehili, Factors influencing the photocatalytic decolorization of Bromophenol blue in aqueous solution with different types of TiO$_2$ as photocatalysts, Desalination, 275 (2011) 224–230.

[37] A. Zuorro, R. Lavecchia, Evaluation of UV/H$_2$O$_2$ advanced oxidation process (AOP) for the degradation of diazo dye Reactive Green 19 in aqueous solution, Desal. Wat. Treat., 52 (2013) 1571–1577.

[38] K. Ouyang, S. Xie, X. Ma, Effect of key operational factors on decolorization of methyl orange by multi-walled carbon nanotubes (MWCNTs)/TiO$_2$/CdS composite under simulated solar light irradiation, Ceram. Int., 39 (2013) 8035–8042.

[39] D.H. Tseng, L.C. Juang, H.H. Huang, Effect of oxygen and hydrogen peroxide on the photocatalytic degradation of monochlorobenzene in TiO$_2$ aqueous suspension, Int. J. Photoenergy, 2012 (2012) 1–9, https://doi.org/10.1155/2012/328526.

[40] C. Yaman, G.A. Gündüz, Parametric study on the decolorization and mineralization of C.I. Reactive Red 141 in water by heterogeneous Fenton-like oxidation over FeZSM-5 zeolite, J. Environ. Health Sci. Eng., 13 (2015) 1–12.